Cracks in Flow liners and their Resolution

I. S. Raju and C. E. Harris[1]

Summary

Cracks were detected in flow liners at the gimbal joints in the LH2 feedlines of the space shuttle's main engines. The cracks initiated at defects in the drainage slots of the flow liners and grew due to high cycle fatigue. Fracture mechanics analyses were conducted to evaluate the life of the liners. These analyses yielded extremely short lives in the presence of small surface or corner cracks. A high fidelity detection method, edge replication, was used to detect the very small cracks. The detected cracks were removed by polishing and the surface quality of the slots was reestablished to improve life of the liners.

Introduction

Cracks were found in flow liners at the gimbal joint in the liquid hydrogen (LH2) feedlines of the space shuttle main engines. Gimbal joints in the LH2 feedlines maintain smooth LH2 flow through the bellows area (see Fig. 1) and into the low pressure fuel pumps and protect the bellows area against flow induced vibration. At the gimbal joints there are two Inconel 718 flow liners – upstream and downstream liners. The liner shells are perforated with numerous slots (see Figs. 1 and 2). The purpose of the slots is to allow access during the manufacturing for clean up and to release the propellant trapped between the flow liner and the bellows.

The initiation and growth of a few cracks in the flow liners was attributed to the combined influence of geometric stress concentrations due to drainage slots, local stress concentrations due to surface roughness produced by the manufacturing processes, residual stresses in the flow liners forming processes and welding of the flange, low cycle fatigue due to thermal stresses from LH2 fill, and high cycle fatigue due to flow-induced loads. As such, a multi-disciplinary team evaluated and studied various aspects of this problem. The flow-physics team investigated cavitation and heat transfer into the flow liner bellows cavity. The computational fluid dynamics (CFD) and flow-physics teams also investigated large scale unsteady motions to the mean flow, back flow, and change in acoustic modes. The loads team, utilizing the flow-physics team's results, developed fatigue loading spectra that the flow liners experience during the entire period of engine flight operation. The damage tolerance team utilized the load spectra to evaluate the life of the liners for several assumed

[1] Structures Discipline Expert and Principal Engineer, respectively, NASA Engineering and Safety Center, NASA Langley Research Center, Hampton, VA 23681, USA.

initial crack sizes and shapes. The fatigue life assessment team devised a Monte-Carlo based simulation of crack initiation assuming that the fluid/structure interactions subject the liners to high cycle fatigue loading.

This paper presents some details of the flow liner problem, the efforts undertaken to understand the problem, and a possible solution to eliminate the cracking.

Flow liner Configuration

Figure 1 presents a schematic of the bellows region and the flow liners. The upstream liner is a cylindrical shell 0.05 in. in thickness and is approximately 12 in. in diameter. The downstream liner is a doubly curved cylindrical shell of approximately the same dimensions. The flow liners are welded to the feedlines and overhang over each other as shown in Fig. 1. Each flow liner contains 38 slots that are separated by a ligament of 0.75 in. (see Fig. 2). Each slot is about an inch long, with a width of 0.25 in.

Development of the Load and Fatigue Spectra

To determine the loads that the flow liners experience, two series of tests were conducted at the NASA Stennis Space center on gimbal joints with flow liners. The flight power levels were simulated in these tests. Extensive strain gage measurements were made and these data were used to infer the loading in the flow liners. In addition, the flow-physics team investigated large scale unsteady motions to the mean flow, back flow, changes in acoustic modes, cavitation, and heat transfer into the flow liner bellows cavity. The loads team, utilizing the results from the flow-physics team and the strain gage data, derived the loading spectra to estimate the load-time history of the liners during flight operations. The team's analyses also identified predominant modes that the liners experience during flight. The predominant mode for the upstream liner is a C9ND mode (C9ND refers to a complex 9-nodal diameter mode, and complex mode suggests both membrane and bending modes act simultaneously), while the downstream liner has 3 predominant modes – 3ND, C4ND, and 5ND. The fatigue loading spectra were determined from these loading spectra and the rainflow method of cycle counting. A typical fatigue spectrum is shown in Fig. 3.

Flow liner Cracks

Figure 2 shows a schematic of the slots in the flow liners and possible crack locations at these slots. Locations A and D are the locations of the axial cracks, and locations B and C are the locations of the circumferential cracks. The welding process results in residual stresses that decrease with the distance from the weld. These stresses were estimated to be 80, 70, 40, and 35 ksi at A, B, C, and D locations, respectively. The inspections of the flow liners located one axial crack at location A growing toward the assembly weld, 5 axial cracks growing toward the free edge from location D, and five circumferential cracks at location B. Analyses have shown that location B has the highest combination of applied and residual stresses. Therefore, location B was chosen for these analyses. Failure in a liner is defined as crack growth across the ligament to a length of 0.6 in. (The difference in lives for c=0.6 in. in comparison to the complete ligament length of 0.75 in. is shown to be negligible [1].) The reason for this failure criterion can be explained as follows. A completely cracked ligament can form a tab, and this tab can break off due to vibratory loads and get ingested into the engine. Such an ingestion can cause catastrophic damage to the engine and the space shuttle.

The 11 cracks found by inspections indicated more crack growth along the outer diameter (OD) than along the inner diameter (ID), suggesting significant bending stresses through the thickness of the liner wall. The manufacturing process created more microscopic damage in the slot surface near the OD. Hence, a reasonable assumption on initial crack shape was a corner crack near the OD edge as shown in Fig. 4. The crack is assumed to grow like a quarter-circular corner crack with (a/c)=1 until it reaches 90 percent of the thickness (i.e until a=0.045 in.) After that point the crack is assumed to grow parallel to the ID until a crack length c=0.3 in. At c=0.3 in., the crack is assumed to transition into a through-the-thickness crack. Newman-Raju equations are used for the stress-intensity factors for quarter-circle corner cracks.

Fracture Mechanics Analyses

With the crack configurations in Fig. 4 and the fatigue spectra, fracture mechanics analyses are conducted to evaluate the life of the liners. Two types of approaches are used to couple the crack growth and the structural dynamics - transfer ratio or factor (TF) approach and the shell-dynamics (SD) approach. They are discussed next.

<u>Transfer factor approach:</u> The TF is the ratio of the strain between a crack location and a measured strain gage location for a specific mode of interest. The TFs are approximate attempts to use the strain gage measurements at mid ligament locations to infer the strain at the crack locations at the edge of the slots and are determined by independent finite element analysis for each specific mode of interest. The TF finite element analysis idealized the liner as a flat plate subjected to membrane and bending loading [1]. The stress-intensity factors are calculated from finite element analyses and then are scaled by the TF. The disadvantage of this method is that the TF is assumed to remain constant as the crack grows, thus over estimating the stress-intensity factor and resulting in conservative estimates of life.

Shell-dynamics approach: To overcome the constraining assumptions involved in the TF approach, an alternate and more rigorous approach is used. In this approach, a three-dimensional/shell finite element analysis couples crack growth kinetics directly to structural dynamics. First, a shell finite element model of a liner with a crack is used to perform the dynamics analysis. The representative mode of excitation in the shell is identified. For this particular shell mode, the strain energy release rates at the crack tip are calculated by scaling the eigen vector of that mode to the strain levels experienced by the liner. The stress-intensity factors are then evaluated from the strain energy release rates. This process is repeated for various crack lengths and various mode shapes.

Crack Growth and Life Calculations

The crack growth and life calculations are performed using NASGRO version 4.11 [2]. Both the TF and SD approaches were used to evaluate the stress-intensity factors. The (da/dN)-ΔK data for Inconel 718 at -423^{0}F obtained in LHe environment are used. A bounding curve that envelopes all the (da/dN)-ΔK data is used in the calculations to provide conservative life predictions. Table 1 presents the predicted life in terms of number of flights as calculated by using the TF and SD approaches. Clearly, the TF approach is more conservative and yields only fraction of a flight life for the upstream liner with an initial crack length of 0.075 in. The SD approach yields longer lives for the upstream liner, but not for the downstream liner.

Table 1: Comparison of predicted life (in flights) using the Transfer Factor (TF) and Shell-Dynamics (SD) approaches

	Upstream Liner, Location B		Downstream Liner, Location B	
c_i, in.	TF Approach	SD Approach	TF Approach	SD Approach
0.075	0.1	21	0.1	0.2
0.020	0.3	39	0.2	1.0

The fracture mechanics-based predictions indicate that the extremely small surface cracks will propagate by high cycle fatigue. To ensure acceptable damage tolerant behavior, these life predictions require detection of extremely small surface cracks below that of traditional non-destructive examination (NDE) methods. As a result, a feasibility study of a high fidelity detection method, edge replication, was conducted. In this method, acetate tape replicas of the slot surfaces were taken from the fatigue specimens that duplicated the slot configuration, flow liner material, and slot processing method. The replicas were taken before and after fatigue cycling. The replicas were then examined under a scanning electron microscope (SEM). Figure 5 shows typical replicas taken from surface cracks. The feasibility study revealed that this method has a resolution of detection of up to 0.001 in. The replica method was then used for crack detection in the slots of the liners in the shuttle fleet. The detected cracks were removed by careful polishing. The liners were then re-inspected for cracks and returned to service.

Concluding Remarks

Cracks were detected in flow liners at the gimbal joints in the LH2 feedlines of liquid propellant engines. The cracks initiated at defects in the drainage slots in the flow liners and grew due to high cycle fatigue. The high cycle fatigue loading is due to interaction between flow-induced loads and structural dynamics. Fracture mechanics analyses were conducted to evaluate the life of the liners. These analyses predicted that extremely small surface cracks would rapidly propagate due to high cycle fatigue. To alleviate this problem, edge replication method was used to detect the cracks. The detected cracks were eliminated and the surface quality of the liners was reestablished by polishing, and the liners were returned to service.

References

1 Harris, C. E. et al., "Orbiter LH2 Feedline Flow liner Cracking Problem", NASA/TM-2005-213787/Version 1.0, NESC-RP-04-11/04-004-E, July 2005, pp. 1-137.

2 NASGRO Version 4.11 Manual, Southwest Research Institute, February 2004.

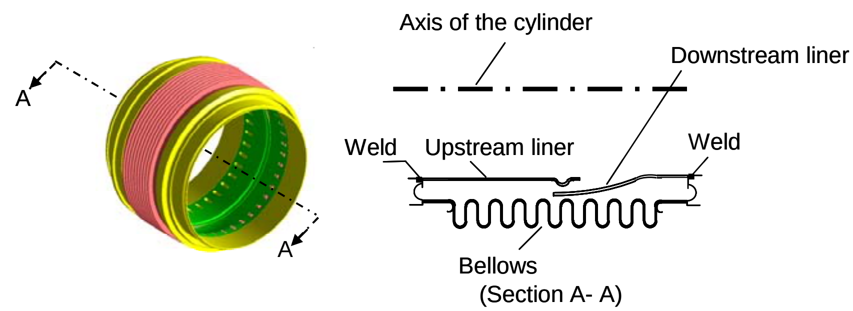

Figure 1: Flow liner configuration (not to scale)

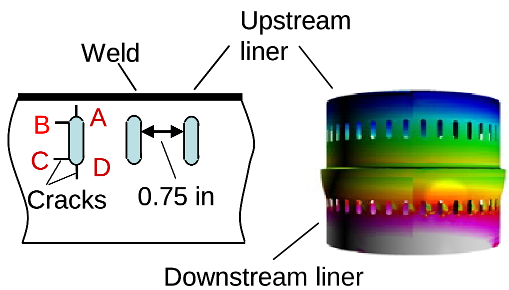

Figure 2: Crack locations at the slots

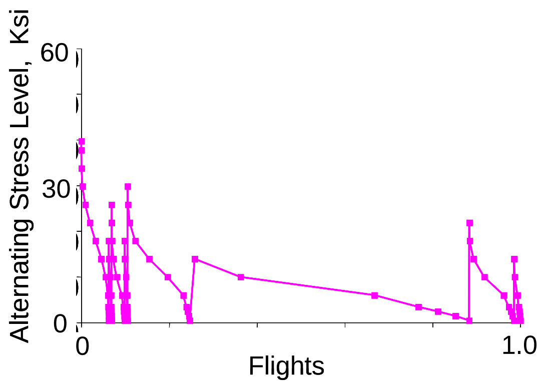

Figure 3: A typical fatigue spectrum

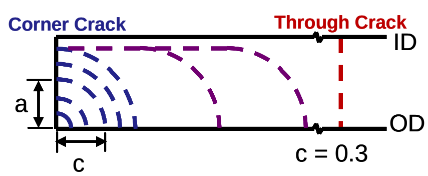

Figure 4: Crack configurations considered

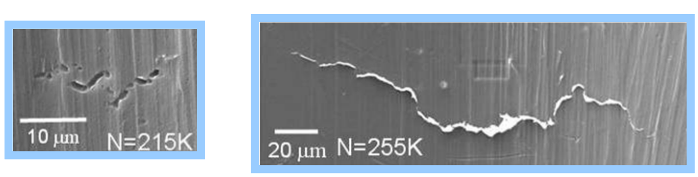

Figure 5: Acetate tape SEM photographs of the same surface crack at 215,000 and 255,000 cycles